INL/CON-19-53232-Revision-2

EGS Collab Earth Modeling: Integrated 3D Model of the Testbed

Ghanashyam Hari Neupane, Robert K Podgorney, Hai Huang, Earl D Mattson, Timothy J. Kneafsey, Patrick F. Dobson, Martin Schoenball, Jonathan B. Ajo-Franklin, Craig Ulrich, Paul C. Schwering, Hunter A. Knox, Timothy C. Johnson, Mark D. White, William Roggenthen, Thomas W. Doe, Douglas A. Blankenship, Vince R. Vermeul, Christopher E. Strickland

September 2019

The INL is a U.S. Department of Energy National Laboratory
operated by Battelle Energy Alliance

INL/CON-19-53232-Revision-2

EGS Collab Earth Modeling: Integrated 3D Model of the Testbed

Ghanashyam Hari Neupane, Robert K Podgorney, Hai Huang, Earl D Mattson, Timothy J. Kneafsey, Patrick F. Dobson, Martin Schoenball, Jonathan B. Ajo-Franklin, Craig Ulrich, Paul C. Schwering, Hunter A. Knox, Timothy C. Johnson, Mark D. White, William Roggenthen, Thomas W. Doe, Douglas A. Blankenship, Vince R. Vermeul, Christopher E. Strickland

September 2019

Idaho National Laboratory
Idaho Falls, Idaho 83415

http://www.inl.gov

Prepared for the
U.S. Department of Energy
Office of Energy Efficiency and Renewable Energy
Under DOE Idaho Operations Office
Contract DE-AC07-05ID14517

EGS Collab Earth Modeling: Integrated 3D Model of the Testbed

Ghanashyam Neupane, Robert K. Podgorney, and Hai Huang

Idaho National Laboratory, Idaho Falls, Idaho, USA

Earl D. Mattson

Mattson Hydrology LLC, Idaho Falls, Idaho, USA

Timothy J. Kneafsey, Patrick F. Dobson, Martin Schoenball, Jonathan B. Ajo-Franklin, and Craig Ulrich

Lawrence Berkeley National Laboratory, Berkeley, California, USA

Paul C. Schwering, Hunter A. Knox, and Douglas A. Blankenship

Sandia National Laboratories, Albuquerque, New Mexico, USA

Timothy C. Johnson, Christopher E. Strickland, Vince R. Vermeul, and Mark D. White

Pacific Northwest National Laboratory, Richland, Washington, USA

William Roggenthen and Nuri Uzunlar

South Dakota School of Mines and Technology, Rapid City, South Dakota, USA

Thomas W. Doe

TDoeGeo, Redmond, Washington, USA

The EGS Collab Team[1]

Keywords

EGS Collab, SURF, Homestake Mine, geothermal, earth modeling

---

[1] J. Ajo-Franklin, T. Baumgartner, K. Beckers, D. Blankenship, A. Bonneville, L. Boyd, S. Brown, S.T. Brown, J.A. Burghardt, T. Chen, Y. Chen, K. Condon, P.J. Cook, D. Crandall, P.F. Dobson, T. Doe, C.A. Doughty, D. Elsworth, J. Feldman, A. Foris, L.P. Frash, Z. Frone, P. Fu, K. Gao, A. Ghassemi, H. Gudmundsdottir, Y. Guglielmi, G. Guthrie, B. Haimson, A. Hawkins, J. Heise, M. Horn, R.N. Horne, J. Horner, M. Hu, H. Huang, L. Huang, K.J. Im, M. Ingraham, R.S. Jayne, T.C. Johnson, B. Johnston, S. Karra, K. Kim, D.K. King, T. Kneafsey, H. Knox, J. Knox, D. Kumar, K. Kutun, M. Lee, K. Li, Z. Li, R. Lopez, M. Maceira, P. Mackey, N. Makedonska, C.J. Marone, E. Mattson, M.W. McClure, J. McLennan, T. McLing, C. Medler, R.J. Mellors, E. Metcalfe, J. Miskimins, J. Moore, C.E. Morency, J.P. Morris, S. Nakagawa, G. Neupane, G. Newman, A. Nieto, C.M. Oldenburg, W. Pan, T. Paronish, R. Pawar, P. Petrov, B. Pietzyk, R. Podgorney, Y. Polsky, J. Pope, S. Porse, B.Q. Roberts, M. Robertson, W. Roggenthen, J. Rutqvist, D. Rynders, H. Santos-Villalobos, M. Schoenball, P. Schwering, V. Sesetty, C.S. Sherman, A. Singh, M.M. Smith, H. Sone, F.A. Soom, P. Sprinkle, C.E. Strickland, J. Su, D. Templeton, J.N. Thomle, C. Ulrich, N. Uzunlar, A. Vachaparampil, C.A. Valladao, W. Vandermeer, G. Vandine, D. Vardiman, V.R. Vermeul, J.L. Wagoner, H.F. Wang, J. Weers, N. Welch, J. White, M.D. White, P. Winterfeld, T. Wood, S. Workman, H. Wu, Y.S. Wu, Y. Wu, E.C. Yildirim, Y. Zhang, Y.Q. Zhang, Q. Zhou, M.D. Zoback

ABSTRACT

The EGS Collab project is conducting a series of stimulation and interwell flow tests in an intermediate scale (~10-20 m) testbed located on the 4850 level in the Sanford Underground Research Facility (SURF) in Lead, South Dakota. The testbed consists of eight ~200 ft (~60 m) HQ-diameter (9.6 cm) boreholes that are drilled into the Poorman Formation from the western rib of the West Access Drift. Of the eight boreholes, one borehole is used as an injection/stimulation well, another sub-parallel borehole located about 10 m away from the injection well is used as a production well, and rest of the other boreholes are used as monitoring wells. For 3D visualization of the testbed as well as to provide spatially accurate and consistent parameter data for geomechanical and geophysical process modeling tasks, we are using Leapfrog Software (Seequent Limited). For analysis of fractures and creation of conditioned stochastic discrete fracture network (CS-DFN) model of the testbed, we are using FracMan (Golder Associates Inc.). As of mid-May 2019, the EGS Collab Leapfrog database contains the general layout of the drifts/shafts at the 4850 and 4100 levels; generalized geologic framework model of a domain that spans both the 4850 and 4100 levels; the CS-DFN of the testbed; and layouts of the EGS Collab testbed boreholes, kISMET testbed boreholes, and other existing boreholes at the 4850 level. This information has been obtained from the SURF Vulcan database, detailed laser scan and point surveys of borehole collar locations, directional surveys of borehole trajectories, and mapping of features in the drifts, boreholes, and cores. Similarly, other types of data that have been incorporated into the Leapfrog database include static features of the testbed such as natural discontinuities (e.g., fractures, weeps), location of monitoring instruments, and stimulation notches. Baseline geophysical characterization results (e.g., seismic, ERT, temperature, etc.) are also imported into the Leapfrog database. The location and size of packers, various point-source signals detected during stimulation and flow tests (e.g., temperature anomalies, micro-earthquake events, etc.) are also compiled in the database. All feature locations are reported using the local Homestake Mine coordinate system. In this paper, we present some of the geostructural characteristics as well as the status of the testbed as represented by Leapfrog/FracMan database/visualizations.

1. Introduction

The United States Geological Survey (USGS) estimates an enormous indigenous renewable energy potential from enhanced or engineered geothermal systems (EGS) in the US (Williams et al., 2008). To realize this potential, the US Department of Energy (DOE) Geothermal Technologies Office (GTO) has initiated a series of EGS programs including Frontier Observatory for Research in Geothermal Energy (FORGE). FORGE is geared towards creating a full-scale field laboratory with a focus on testing and validating technologies to improve EGS reservoir access, creation, and sustainability. As a bridge to the FORGE initiative, the DOE-GTO is also funding a research project – the EGS Collab Project– to create an intermediate-scale reservoir in an underground facility that provides a more accessible reservoir for refining our understanding of rock mass response to stimulation, testing novel monitoring tools, and validating thermal-hydrological-mechanical-chemical (THMC) modeling approaches (Dobson et al., 2017; Kneafsey et al., 2019a,b).

The Sanford Underground Research Facility (SURF) was selected as a site for the EGS Collab Testbed (Dobson et al., 2017). SURF is a dedicated underground research facility using the extensive network of tunnel systems developed over a century of gold mining

activities as the Homestake Gold Mine in Lead, South Dakota (Heise, 2015). Recently, this facility hosts several physics, astrobiology, and geosciences laboratories and testbeds.

For geologic framework modeling, fracture mapping, creating discrete fracture models, and exporting fractures as well as rock-property-based discrete as well as simple meshed models for additional process modeling tasks, the EGS Collab project is using both Leapfrog (Seequent Limited) and FracMan (Golder Associates, Inc.). In this paper, we present geologic model, testbed boreholes, natural fractures, weep zones, and a conditioned stochastic discrete fracture network (CS-DFN) model developed for the testbed. We present an approach of the Leapfrog/FracMan refined fracture model being used for 3D fracturing modelling. Finally, we have also included conceptual models of the hydraulic fractures and their intersections with natural fracture zones/weeps, and representative flow paths in the testbed.

2. EGS Collab Testbed

2.1 Underground Location

The testbed is located on the western rib of the West Access Drift of the 4850 Level (4850 feet below ground surface) at SURF (Figure 1), nearby the kISMET testbed (Oldenburg et al., 2016). The testbed is accessible via the Yates Shaft and the Ross Shaft. Once on the 4850 level, the site can be reached directly through the West Access Drift or via the East Drift and South Drift. The site is well ventilated and provided with electricity, internet, lighting, running water, drainage, and so on.

2.2 Geologic Model

SURF is developed at the former Homestake gold mine site in the Black Hills of South Dakota, where active mining took place for over a century. Over the years, the area was subjected to metamorphism, basic and felsic intrusions, and orogenic events. Subsequently, the area was uplifted to form the Black Hills at about 530 Ma. Younger volcanic activity (e.g., Tertiary) also emplaced a series of rhyolitic dikes into the rock formations in vicinity of the testbed (Caddey et al., 1991; Frei et al., 2009).

A simplified geologic framework model was developed for a domain that contains testbed and beyond (Figure 2). The geologic model is developed using information acquired from previous geologic mapping of the area (e.g., Caddey et al. 1991) and geological mapping/modeling of SURF for various underground laboratory spaces and tests (e.g., Lisenbee and Terry, 2009; Hart et al., 2014). Since the testbed is entirely located outside of the Vulcan (Maptek Pty Ltd) based conical 3D geological model developed by Hart et al. (2014), we primarily used geologic data from Lisenbee and Terry (2009) to create the testbed geologic model (Figure 2). The generalized geologic model includes of four units: the lower Yates member of the Poorman Formation (amphibolite), the upper Ross member of the Poorman Formation (metasedimentary phyllite), the Homestake Formation, and Tertiary rhyolite dikes.

The Yates member is an amphibolite metabasalt consisting of hornblende and plagioclase (Caddey et al., 1991), and is cross-cut by calcite veins (Caddey et al. 1991). Along with these calcite veins, local oxidized sulfide layers define zones of weakness in the rock. The Ross member of the Poorman Formation (referred to here as the Poorman) consists of graphitic sericite-biotite phyllite/schist with local interlayers of quartz, and calcite veins (Caddey et al. 1991; Steadman and Large, 2016). This unit shows intense folding with small crenulations to mesoscale folds. The testbed is entirely located within this formation. The Homestake

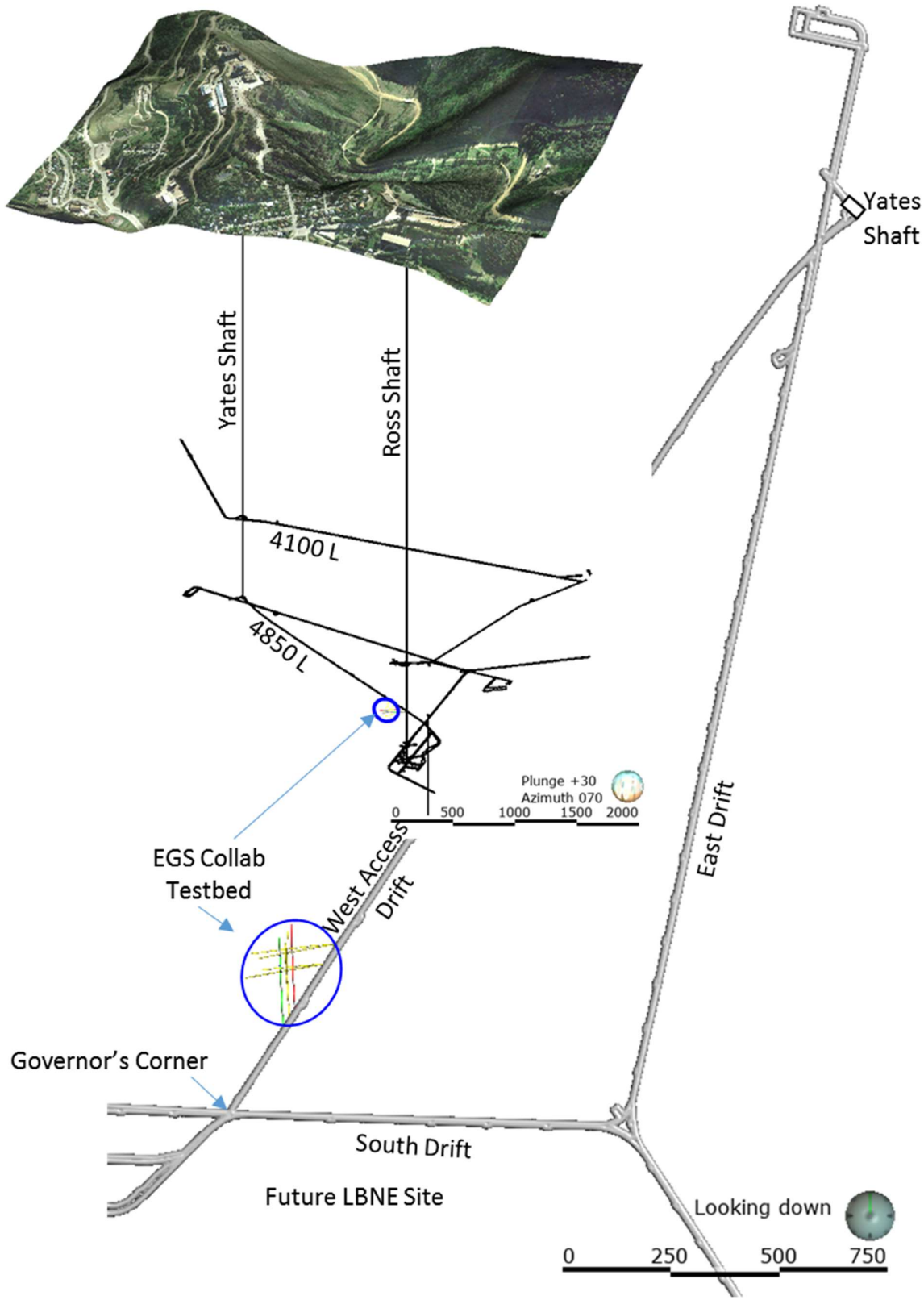

Figure 1. Location of EGS Collab testbed at the Sanford Underground Research Facility in Lead, SD.

Formation is the primary gold-bearing unit in the area. It is an early Proterozoic banded iron formation that has gold deposits in association with sulfide mineralization (Caddey et al., 1991).

Tertiary rhyolite dikes intersect all other units within the geologic model domain. In our geologic model, the rhyolite dikes are represented by a NW-SE striking continuous unit northeast from the testbed; however, rhyolite dikes occur as a few centimeters to tens of meters thick separate and interconnected units (swarms). The rhyolite dikes are aphanitic in texture with scattered sanidine phenocrysts (Caddey et al., 1991). Structurally, the EGS Collab testbed is located on the west limb of the plunging Lead anticline structure.

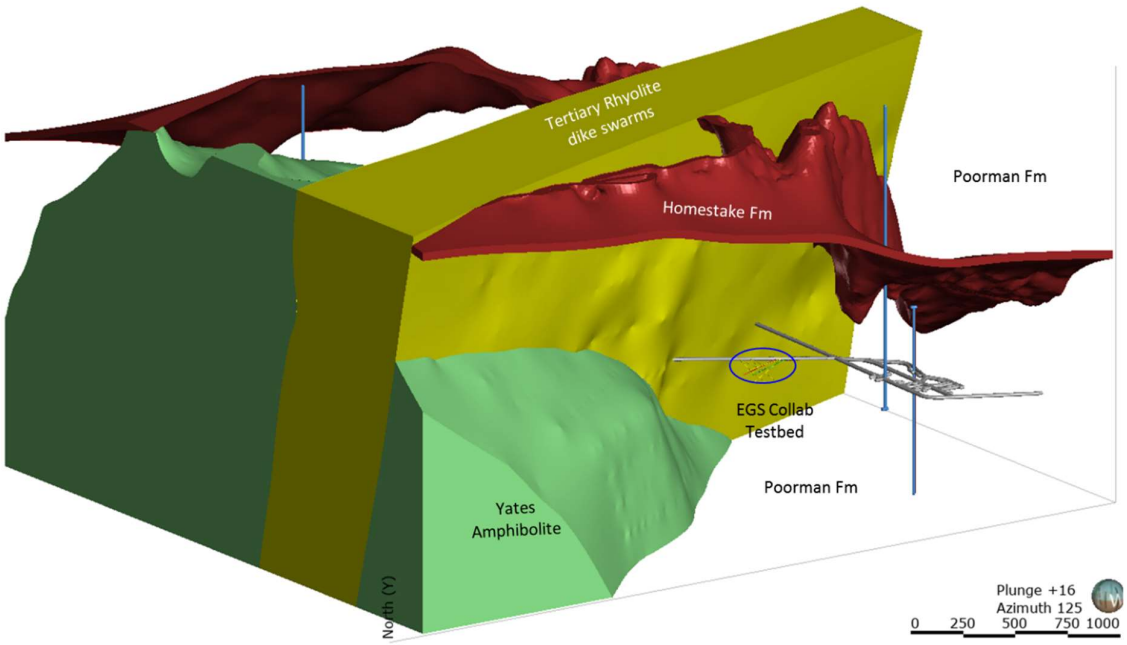

Figure 2. Generalized geologic framework model of the EGS Collab testbed and surrounding area.

In addition to the units depicted in Figure 2, (Yates, Poorman, Homestake, and rhyolite dikes), additional rock units in the area are the Ellison, Northwestern, Northwestern Amphibolite, Flagrock, Flagrock Amphibolite, and Grizzly Formations. Detailed geologic descriptions of these units can be found elsewhere (e.g., Caddey et al., 1991).

2.3 Testbed Boreholes

The EGS Collab Experiment-1 (E1) testbed consists of eight HQ-diameter (9.6 cm), continuously cored sub-horizontal holes with a nominal length of about 200 ft (Figure 3a). Each hole was steel-cased to a depth of 20 ft from the top (collar). Six of the boreholes (E1-OT, E1-OB, E1-PST, E1-PSB, E1-PDT, and E1-PDB) are intensively instrumented with various equipment for seismic, temperature, electrical resistivity monitoring (Figure 3b), and were grouted with a mixture of ground blast furnace slag, ground pumice, and Portland cement. The remaining two holes (E1-I and E1-P) remained open and being used as stimulation and production wells. Five notches were created at different depths along the E1-I to facilitate stimulation and help initiate intended hydraulic fracturing (Morris et al., 2018).

The layout of the testbed boreholes was designed to create stress-field controlled hydraulic fracture(s) and to provide the maximum opportunity to characterize/monitor fracturing event(s) (Knox et al., 2017). The injection well (E1-I) and production well (E1-P) were drilled (nominal azimuth = 356˚ and inclination = 12˚) approximately parallel with the trend of minimum horizontal stress (trend = 356˚ and plunge = 9.3˚) in the area (which was previously determined at a nearby kISMET testbed (Oldenburg et al., 2016) with intended hydraulic fracture striking N86˚E with a dip of 81.7˚ (as depicted by the disk at the 164-notch in Figure 3a) along the maximum horizontal stress. The two boreholes (E1-OT and E1-OB) are designed as nearby monitoring holes orthogonally intersecting the intended hydraulic fracture. Other four monitoring holes (E1-PST, E1-PSB, E1-PDT, and E1-PDB) are designed as being shallow and deep wells that are intended to be parallel to the hydraulic fracture (White et al., 2017; Knox et al., 2017).

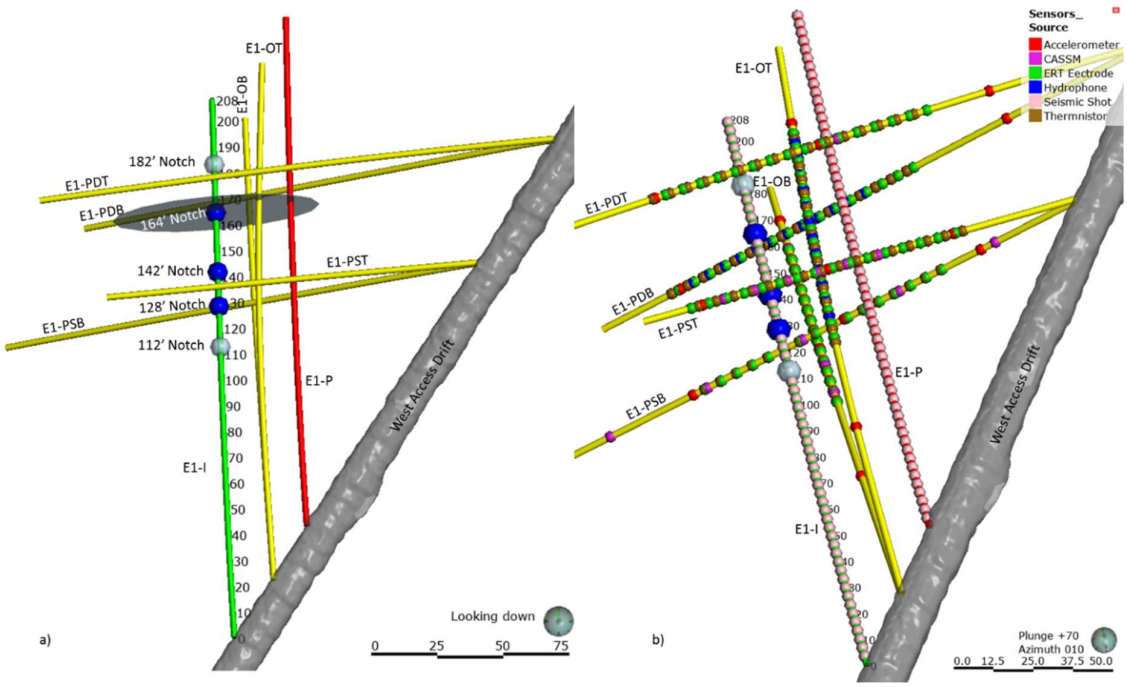

Figure 3. a) Layout of boreholes in the testbed. Six boreholes (yellow lines) are used as monitoring wells, one borehole (green line) is used as an injection/stimulation well, and the remaining borehole (red line) is used as a production well. The three dark blue spheres along E1-I are stimulation notches where some stimulation activities have been performed, and the two light blue spheres are additional notches that have yet to be stimulated. The large disk at the 164 notch represents the expected (controlled by a stress field as measured at the nearby kISMET testbed, Oldenburg et al., 2016) hydraulic fracture striking N86˚E with a dip of 81.7˚. b) Locations of various geophysical sensors in boreholes (Schoenball et al., 2019; Johnson et al., 2019). The seismic shot/receiver locations along E1-I and E1-P were used for a one-time cross-borehole seismic survey (Schwering et el., 2018).

2.4 Natural Discontinuities in the Testbed

Although the results of nearby kISMET testbed (where the vertical boreholes were used to characterize the testbed and conduct stress measurement tests) indicated the presence of limited natural fractures in the area, several field studies and current testbed core inspections and interpretation of borehole imaging indicate the existence of several structural discontinuities in the current testbed (Figure 4a). Structural mapping of the drifts conducted

during the site selection process revealed several weeps along the West Access Drift (Roggenthen et al., 2018; Ulrich et al., 2018). These weeps are characterized by drips, wet surfaces, mineral deposits, and evaporative crusts (Figure 4b). Natural fractures in the testbed have a general NW-SE strike and steep dip (trend/plunge of the mean pole is 51˚/2.5˚). All weep zones in the drift have similar strikes with near vertical dip. Structural attributes of weeps and natural fractures in the testbed are similar to the attitude of the rhyolite dikes located to the NE from the testbed (Figure 2).

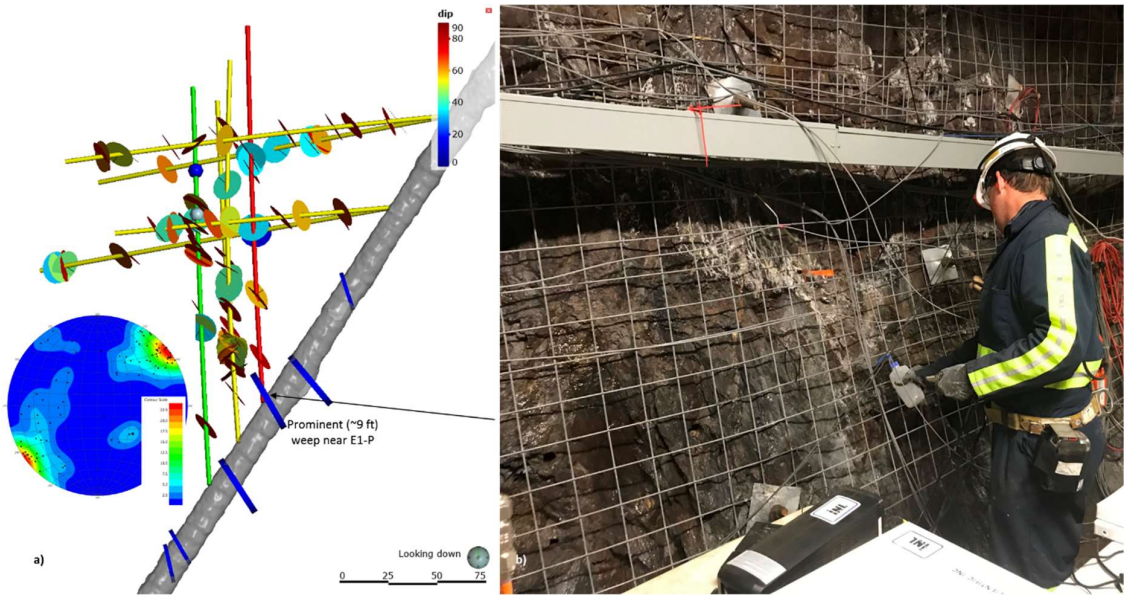

Figure 4. a) Fractures and weep identified along the testbed boreholes and West Access Drift in the vicinity of testbed. Natural fractures dominantly have a NW-SE strike, and are steeply dipping (hot colored disks are steeper). The size of the disks are for illustrative purposes only. Large/thick blue disks are weeps, which also share the common NW-SE strike of the natural fractures observed along the boreholes. b) A photograph of a prominent weep on the drift rib near E1-P. The grey-white materials on the photograph are mineral deposits and evaporation crusts. The apparent thickness of this weep is about 9 ft. In the photograph, Luke Frash (LANL) was constructing a weep water collection ledge on April 26, 2019.

Originally, it was expected that the current testbed boreholes have no or minimum hydraulic connectivity from each other or to the drift. During early core inspection and a find-the-fracture exercise (low pressure injection over the entire length of each hole at a time), a few hydraulically connected zones and flowing fractures were identified (Roggenthen et al., 2018; Ulrich et al., 2018). For example, two such features are the OT-P Connector, a hydraulically connected fracture system associated with OT-161 (fracture naming system: name of the hole and depth at which the fracture is located), and the P-122 natural fractures. Similarly, Roggenthen et al. (2018) extended a prominent weep near E1-P (as pointed in Figure 4) into the E1-P and E1-OT based on the fracture rich, vuggy cores in the projected segment of the boreholes. Over the course of several hydraulic fracturing and flow tests activities, it became obvious that the testbed has (or has the tendency to have) substantial cross-borehole connectivity through already existing hydraulic connectors or activated natural fracture zones.

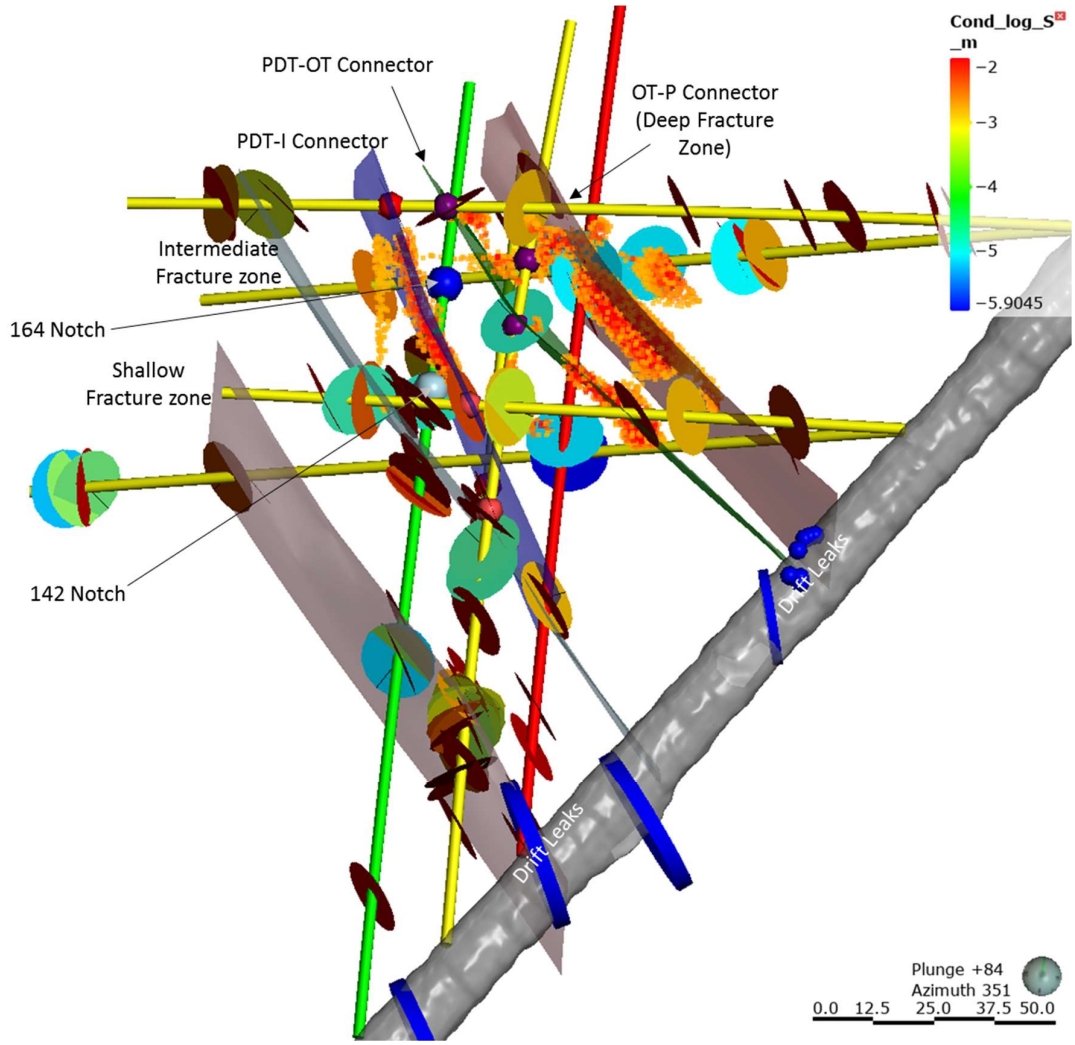

Figure 5. Natural fracture zones (or weeps) in the testbed. At least five fracture zones or weeps are identified in the testbed. Large purple spheres are temperature anomalies noticed during the 164-notch activities (stimulation and flow tests) whereas large red spheres are temperature anomalies noticed during the 142-notch activities (stimulation and flow tests) or entire whole pressurization after the 142-notch stimulation.

Figure 5 illustrates the current state of natural fracture zones in the testbed. These fracture zones are represented by one or more natural fractures, vuggy rocks, and sheared features, and they are either naturally hydraulically connected or became conductive during multiple stimulations and subsequent flow tests. As mentioned above, the hydraulic conductivity of the Deep Fracture zone was identified during the find-the-fracture exercise as the OT-P Connector. The natural hydraulic connectivity of this fracture zone was established in such a way that when E1-OT was pressurized (low pressure entire hole injection), a flow of water was noticed from a natural fracture at 121.75 ft along E1-P, and when the injection was reversed, a flow was noticed from a natural fracture at 161.58 ft in E1-OT. A segment of the Shallow Fracture zone was first recognized by Roggenthen et al. (2018) based on weep mapping and core inspections. This fracture zone has a prominent weep near E1-P that extends to E1-P and E1-OT, and likely continues in an incipient fashion to E1-I and beyond. During flow tests after stimulation at both the 164-notch and the 142-notch, water seepage

was noticed from the weep near E1-P. This seepage of water was likely to have routed to E1-OT at depth to the intersection of E1-OT and the Shallow Fracture zone (at depth of 42 to 53 ft along E1-OT) and to the weep on the drift rib (Figure 16c). Since the top 20 ft section of E1-P (as well as all other boreholes) is steel-cased, the production hole did not channel this water to the drift. Based on the distribution and nature of fractures, and distribution of high electrical conductivity ERT cells, the Intermediate, PDT-I Connector, and PDT-OT Connector fracture zones were suspected to exist. The presence and their subsequent activation were later verified by the distribution of microseismic clouds, temperature anomalies, and flow patterns during stimulation and flow test activities associated with both the 164-notch and the 142-notch. Recent slip tendency analysis also suggests the propensity of these fracture zones for shear activation during the stimulation and flow tests (Singh et al., 2019).

3. Discrete Fracture Network Model

3.1 CS-DFN for the Testbed

A conditioned stochastic discrete fracture network (CS-DFN) model was created for the testbed following a workflow illustrated in Figure 6. A similar approach was also adopted to create a CS-DFN for the EGS FORGE site in Milford, Utah (Finnila et al., 2019). The workflow begins with the selection of a model domain that is populated with a stochastic DFN. A domain size of 250 ft ×250 ft × 125 ft (Figure 7) was used to create a stochastic DFN model for the testbed. This model domain entirely encompasses the testbed boreholes, and is located within the Poorman Formation.

A. Define DFN Region/Model Domain
B. Define Deterministic Fracture Set
C. Define Stochastic Fracture Set
   - Intensity
   - Orientation
   - Size
   - Shape
D. Generate Stochastic Fractures
E. Find Stochastic Fractures Intersecting Wells and Remove
F. Generate Deterministic Fracture Set Intersecting Wells
G. Combine Remaining Stochastic Fractures [E] and Deterministic Fractures [F]
H. Export Conditional Stochastic Fractures [G]

Figure 6. Generalized workflow employed to create a conditioned stochastic DFN model for EGS testbed. [Note: In step 3, fracture termination, aperture size, compressibility, and permeability of the fractures can be defined. However, in the current DFN model, these fracture attributes have not been defined.]

Fractures along the boreholes (Figure 4a) were identified and their orientations were determined by interpreting acoustic/optical televiewer logs and core inspections. The majority of the fractures in the boreholes are classified as open fractures and a small number of healed (some of the healed fractures might have pin-holes, small vugs, and partial openings) fractures are also included in the fracture dataset. These fracture data were used to create basic fracture statistics (e.g., intensity as P10 for each hole). The P10 (number of fractures per unit length) values of the testbed boreholes range from 0.04 to 0.12 fracture per foot (Figure 8a). Figure 8b shows the size distribution statistics used to populate stochastic fractures in the model domain. The size distribution statistics were refined using the data included in ARUP (2015) and observational data from the current testbed.

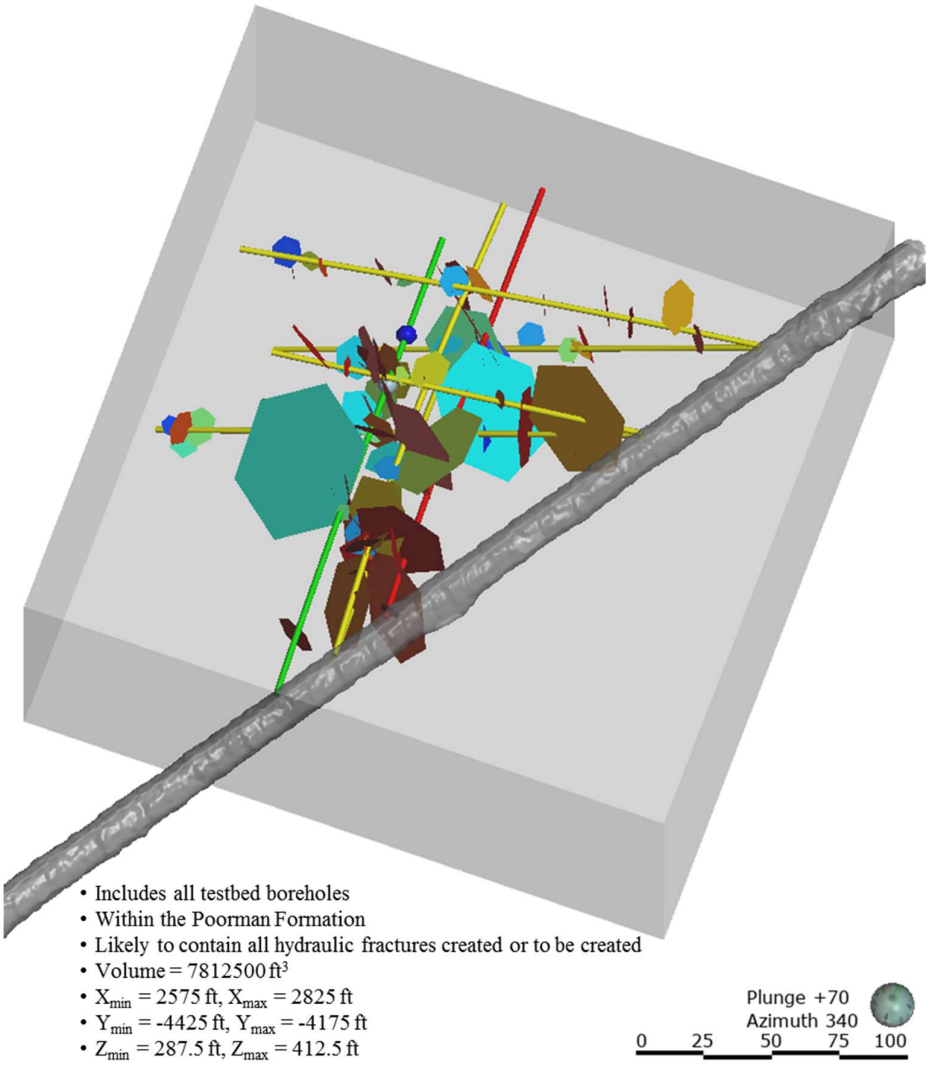

Figure 7. CS-DFN Model domain of testbed. The model domain is 250 ft ×250 ft × 125 ft. The depicted fractures along the holes are deterministic in their locations (the point of fracture-borehole intersection) and orientation (bootstrapped) but their sizes (Log Normal distribution) are stochastically defined in FracMan.

Hole ID	Interval	P10 (1/ft)
E1-I	Full Length	0.07
E1-P	Full Length	0.06
E1-OT	Full Length	0.12
E1-OB	Full Length	0.04
E1-PST	Full Length	0.09
E1-PSB	Full Length	0.04
E1-PDT	Full Length	0.07
E1-PDB	Full Length	0.04

a)

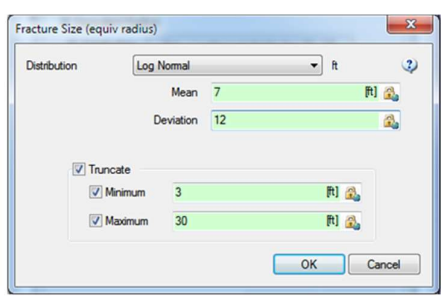

b)

Figure 8. a) Calculated P10 values of testbed boreholes. b) Size distribution parameters used to create stochastic DFN.

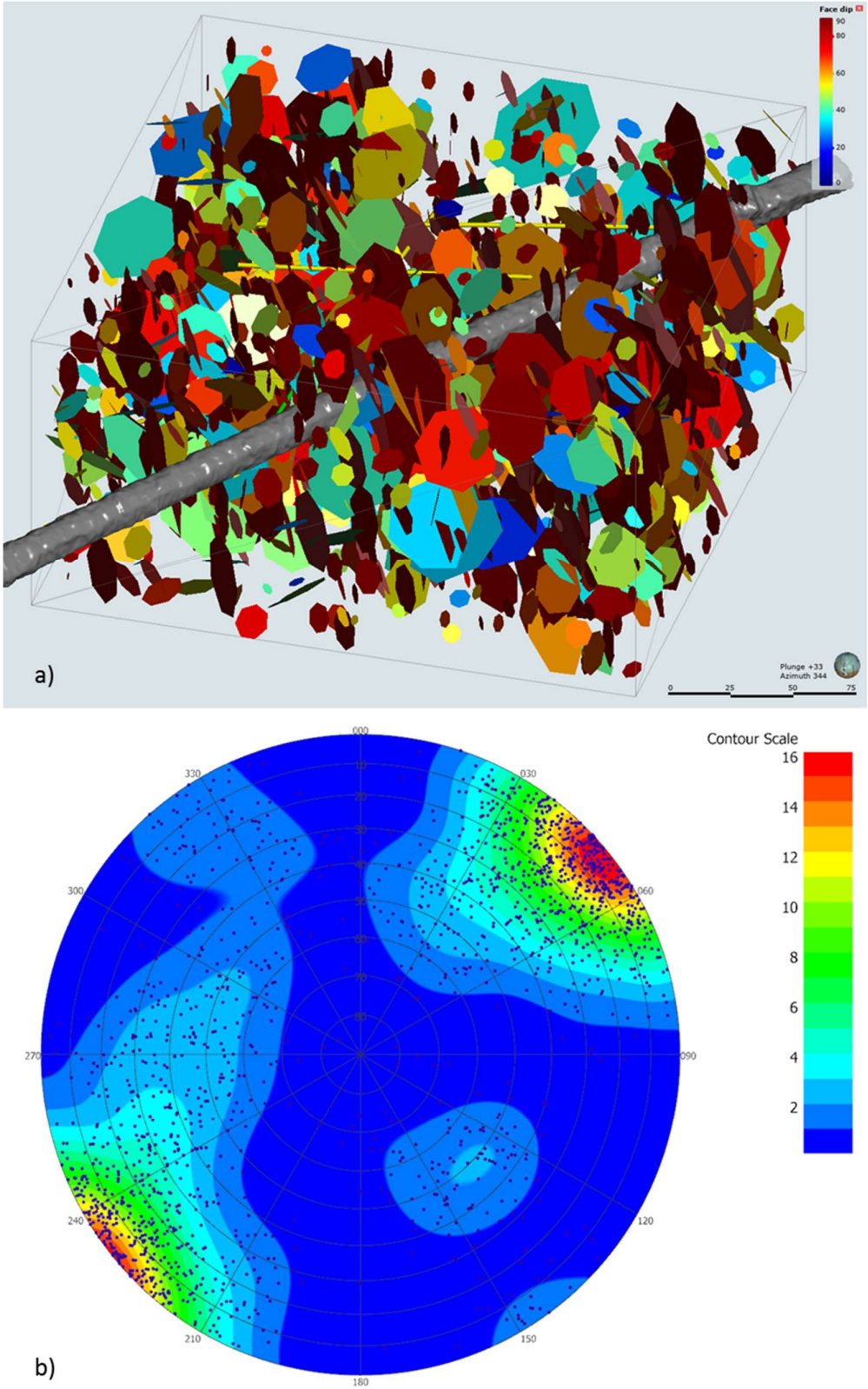

Figure 9. a) Conditioned stochastic DFN model for EGS Collab testbed. b) Stereonet pole plot of the DFN model fractures.

Orientations of the stochastic fractures are "bootstrapped" to the orientations of known fractures (Figure 4a) in the testbed. In FracMan, bootstrapping helps match the orientation pattern and proportions of stochastically created fractures exactly or with assigned "fuzziness" with a concentration parameter with that that of known fractures.

Finally, the CS-DFN model (Figure 9) for the EGS Collab testbed is created following steps D through H in Figure 6.

3.2 DFN for 3D Modeling of Hydraulic Fracturing

Recently, a sub-domain (representing the 164-notch in E1-I) of the overall CS-DFN model domain was selected for 3D modeling of hydraulic fracturing (Huang et al., 2019). This small sub-model domain is illustrated in Figure 10. Additionally, for computational efficiency of the 3D hydraulic fracturing simulations, fractures in this sub-model were greatly simplified by removing small fractures and those not intersecting with any other fractures and wellbores. The natural fracture representing the OT-P connector was retained in the 3D hydraulic fracture model (Huang et al., 2019). The result of this 3D hydraulic fracture modeling is given in Figure 11. Additional details of this work can be found in Huang et al. (2019).

Figure 12 shows the major natural fracture zones and domain size selected for the next phase of 3D fracture modeling. This refined natural fracture model along with the embedded rock mass are currently being used to create a seamless mesh for this task.

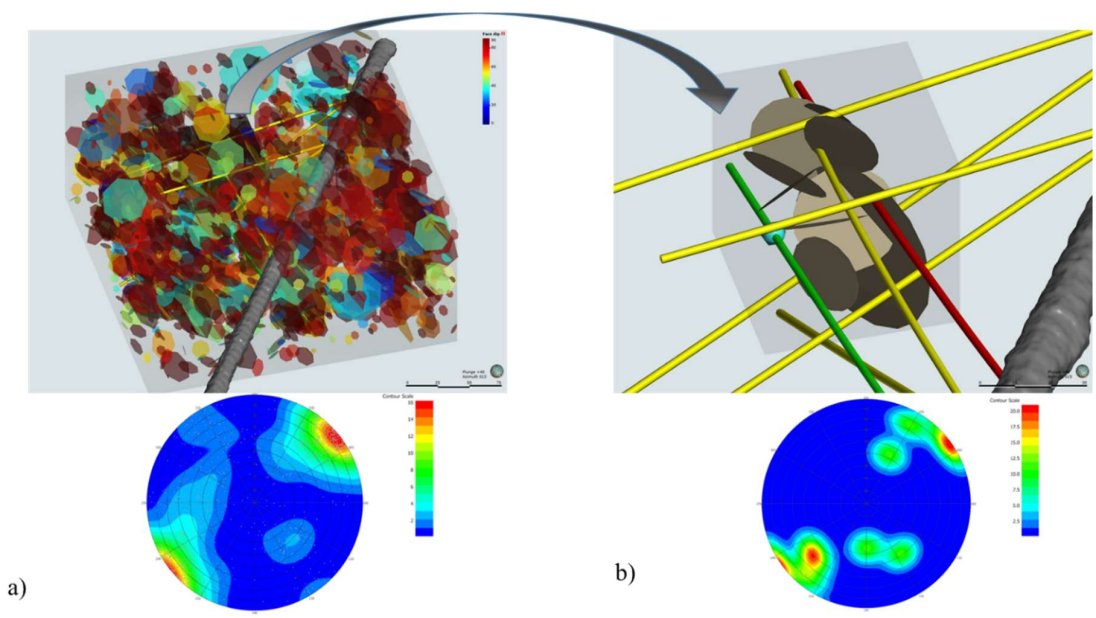

Figure 10. a) Conditioned stochastic DFN model with a small sub-domain encompassing the 164-notch and region around it. b) 3D hydraulic fracture model domain (marked as light gray box) along with selected natural fractures. For simplicity and computational limitations, non-intersecting fractures with radius <5 ft were discarded for 3D hydraulic fracture model (Hunag et al., 2019).

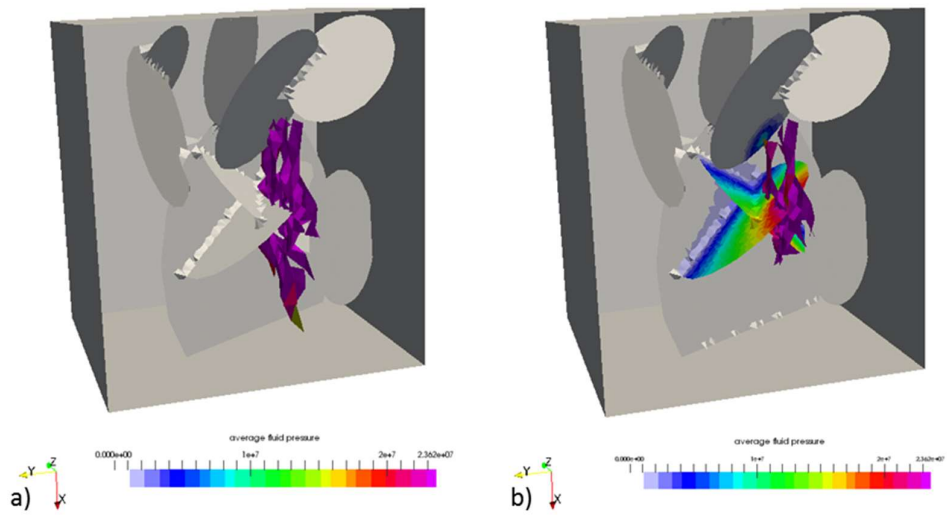

Figure 11. Simulated fracturing patterns in 3D. a) DFNs with permeability and mechanical properties similar to rock matrix, and b) DFN permeability is four times higher than the rock matrix and the DFN tensile strength is 1/10 of the rock matrix. Rock matrix permeability = 10^{-19} m^2 (Frash et al., 2019), and rock matrix tensile strength = 5 MPa, horizontal minimum stress = 21 MPa, in situ horizontal maximum stress = 31 MPa, vertical stress = 41 MPa (Huang et al., 2019).

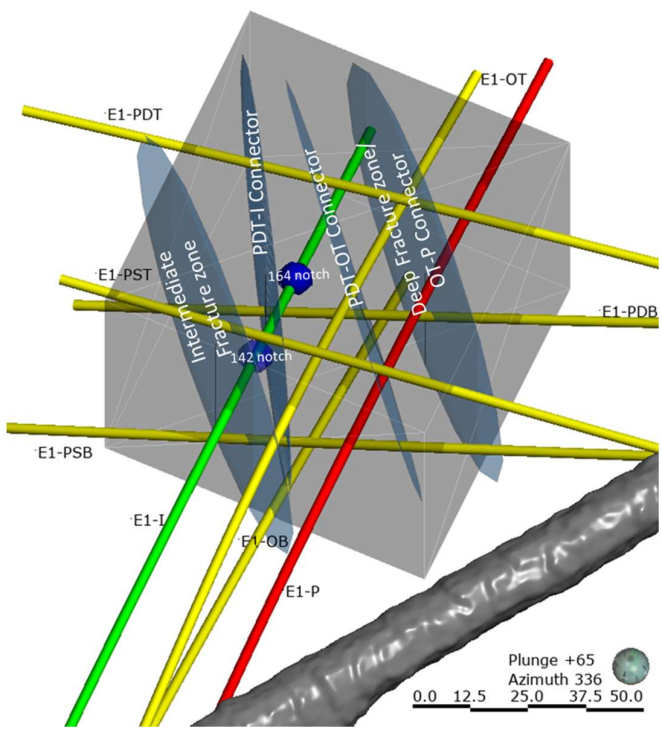

Figure 12: Major natural fracture zones and model domain selected for next 3D hydraulic fracturing simulation.

4. Baseline Geophysical Characterization

Some early geophysical characterizations of the testbed as well as stimulation/flow tests and induced micro-earthquakes (MEQ) events were imported to Leapfrog. In this section, we present Leapfrog visualization of cross-borehole seismic characterization and baseline ERT results of the testbed. Seismic (Schwering et al., 2018) and electrical resistivity tomography

(ERT) (Johnson et al., 2019) surveys were employed to characterize the testbed. These geophysical surveys and modeling results helped understand and define the baseline state of the testbed and are critical for providing testbed-specific model parameters to monitoring efforts (e.g., real-time MEQ), and identifying changes induced by stimulation and flow tests in the testbed.

4.1 Cross-borehole Seismic Characterization

The cross-borehole seismic survey was conducted using a seismic array consisting of both temporarily deployed sources and receivers along E1-I and E1-P and permanently deployed hydrophones in the monitoring holes (Schwering et al., 2018). The locations of shot points and hydrophones at various depths along E1-I and E1-P, and locations of hydrophones/accelerometers are shown in Figure 3. Figures 13 and 14 show 2D (plane of injection-production wells) and 3D baseline P-wave and S-wave velocity models (Schwering et al., 2018). The testbed is anisotropic in terms of both P-wave and S-wave velocities. In general, the variation in seismic velocities on the E1-I – E1-P plane (Figure 13) seems to mimic the overall NW-SE trending structural grain (Figure 5) of the testbed. However, the 3D P-wave velocity model reveals a strong east-west variation in velocities with some distortion imprinted by the NW–SE trending structural features (Figure 14). For additional details, we refer to Schwering et al. (2018).

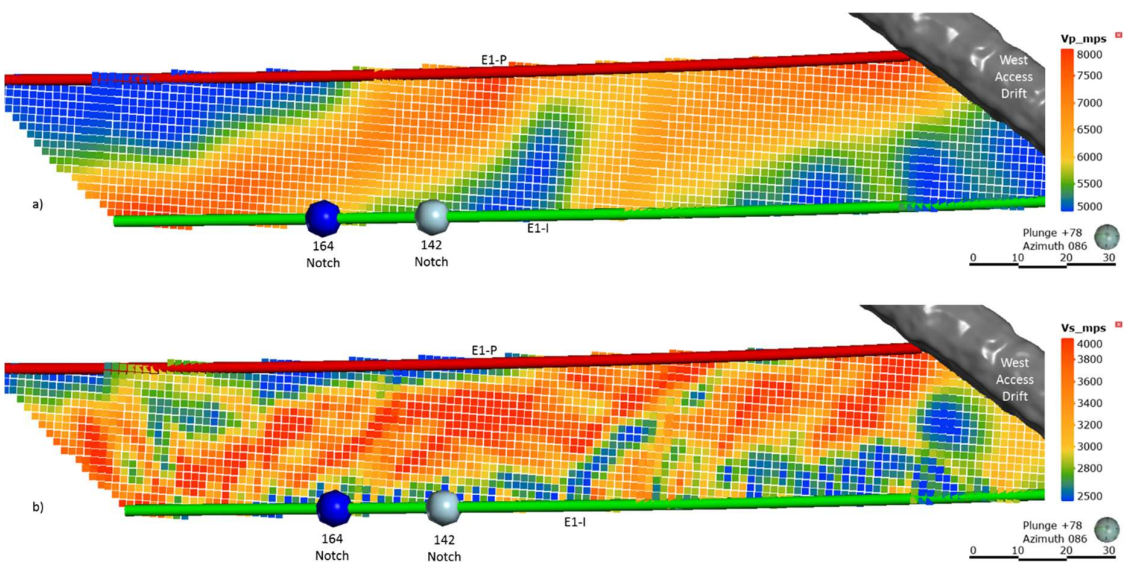

Figure 13. a) P-wave velocity and b) S-wave velocity 2D (I-P plane) models of the testbed (Schwering et al., 2018).

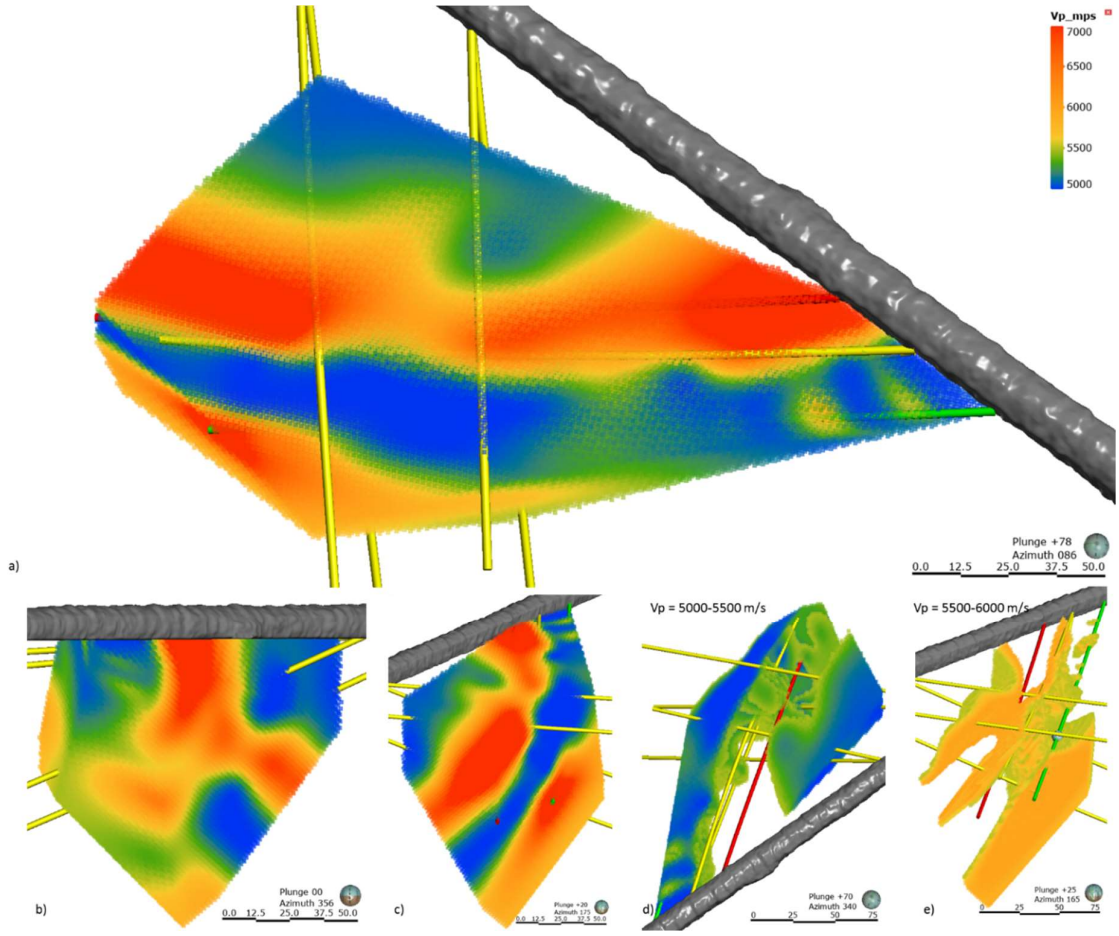

Figure 14. 3D P-wave velocity model of the testbed (a-c). d) and e) depict low velocity (P-wave) zones in the testbed (Schwering et al., 2018).

4.2 Baseline ERT Characterization

Baseline, time-lapse, and real-time ERT surveys of the testbed were conducted using an array of electrodes deployed in the monitoring wells (Figure 3). The ERT array consists of 16 electrodes in each of the 6 monitoring holes encompassing the expected hydraulic fracture zones (Johnson et al., 2019). The baseline ERT model (Figure 15) shows that the testbed consists of highly heterogeneous rock fabric with a range of four orders of bulk electrical conductivity magnitude. The alternating distribution of high and low bulk electrical conductivity zones closely mimics the distribution of fractures and weeps (Figure 5) in the testbed (Johnson et al., 2019). For additional details, we refer to Johnson et al. (2019).

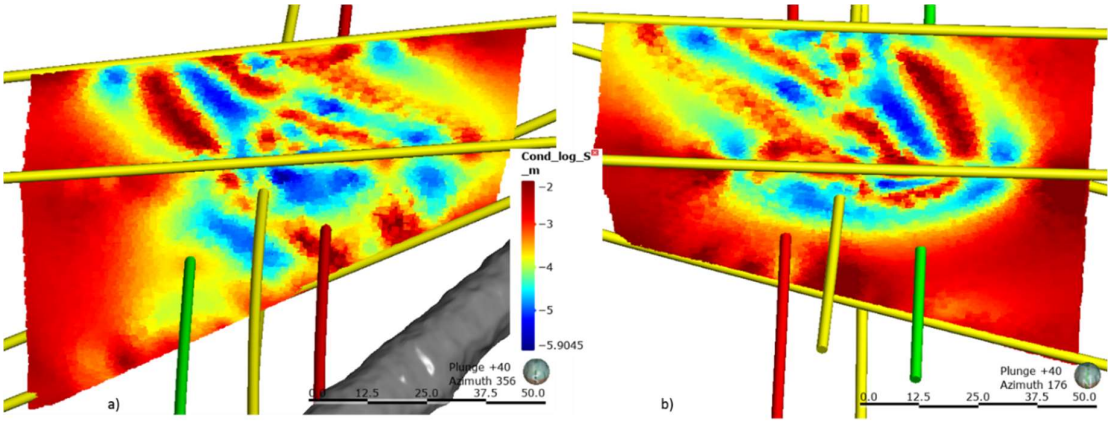

Figure 15. Baseline ERT model of the testbed (Johnson et al., 2019).

5. Conceptual Flow Models of the Testbed

Various stimulation/flow tests conducted in the testbed have been very informative to develop and refine conceptual hydraulic architectures of the testbed over time. Summarized descriptions of major stimulation and flow tests conducted in the testbed can be found in (Kneafsey et al., 2019a; White et al., 2019; Fu et al., 2019).

5.1 Conceptual Flow Models: 164-Notch

Table 1 provides the injection rate and outflow rates for different producers during the October-November, 2018 tests. Observational data (e.g., MEQ, DTS, etc.) combined with dominant flow patterns and fracture systems (Figure 5) in the testbed are used to create a series of diagrams (Figures 16 and 17) to illustrate the evolution of flow patterns in the testbed.

Table 1. Injection rate and outflow rates from different sources.

In/Outflow rates (mL/min)	October						November				
	24	25	26	29	30	31	1	7	8	9	14
Injection	400	400	400	800	800	400	400	400	400	400	400
PI Flow	81	124	120	170	181	75	70	35	30	29	26
PB Flow	60	118	123	200	167	82	85	40	40	41	54
OT Flow	16	27	26	40	30	9	10	118	113	130	190
PST	0	57	66	25	67	40	40	15	12	11	11
PSB	0	0.3	0	NA	NA	2	0	0	0	0	NA
PDT	0	1.3	2.1	95	180	78	78	10	5	NA	4
PDB	0	2.2	2.5	4	14	6	4.4	2.5	0	NA	1
OB	0	0.7	0.7	NA	NA	0	0	0	0	0	1
Total Outflow	157	330	340	534	639	292	287	221	200	211	287
Recovery %*	39	83	85	67	80	73	72	55	50	53	72

* These calculations do not account the leaks that occurred from rock bolts on the rib and back of drift (Figure 16a-b). Out of several drip points, one dominant leak was producing about 10 mL/min outflow on October 26, 2018.

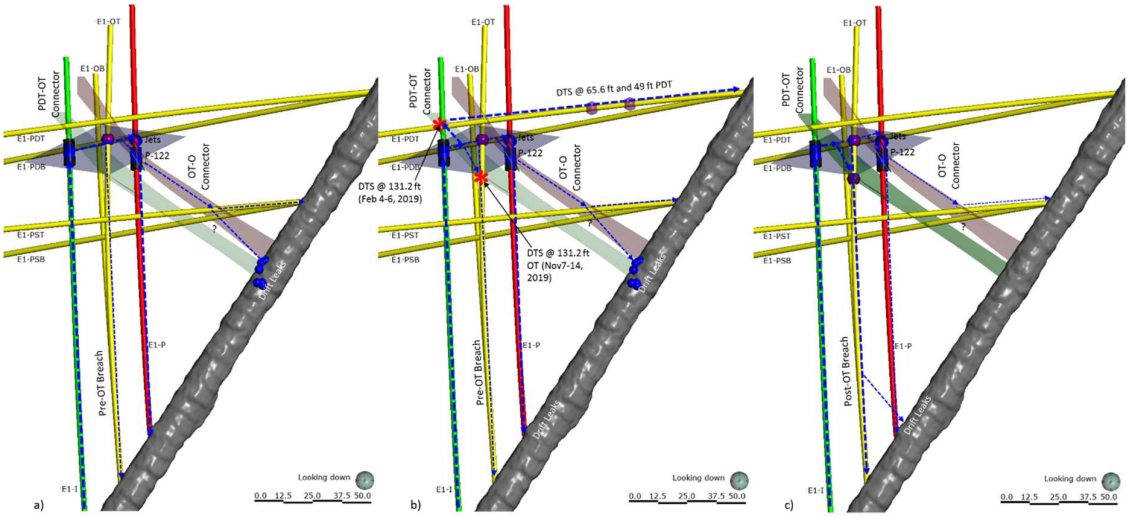

Figure 16. Major outflow sources and interpreted likely flow paths. a) October 24-29 (early morning), 2018. Dominant outflows were PB, PI, and PST with a small leak from OT (Table 1). Drift leaks were noticed from several rock bolts on the rib and back of drift in a section 30-40 ft from E1-PST to E1-P; b) October 29 (afternoon) to November 1, 2018. Major outflows were PDT, PB, and PI, and PST, and PST with small flow from OT (Table 1); and c) November 7-14, 2018. Major flows were OT, PI, and PB with small flow from PST. Purple spheres are locations of temperature anomaly.

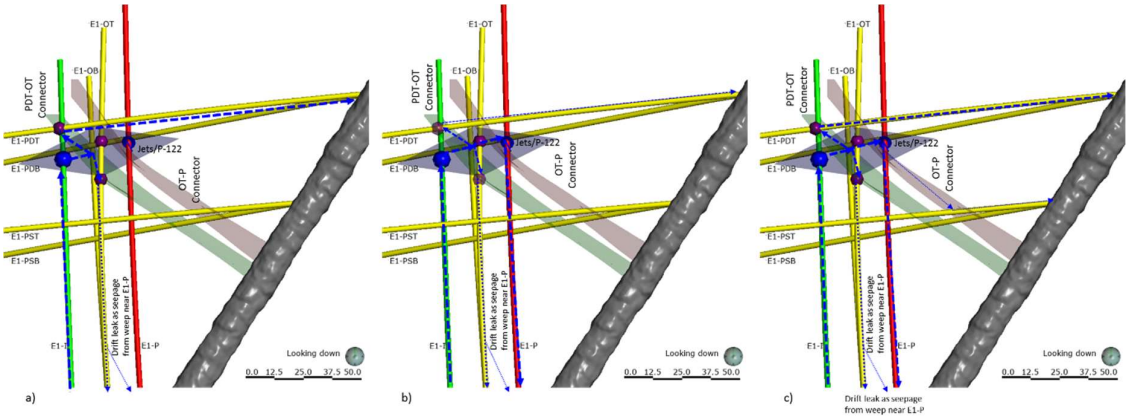

Figure 17. Major outflows patterns observed during third set (February-March, 2019) of hydraulic characterization tests at the 164-notch. a) E1-PDT was the main producer during February 4-6, 2019. No flow detected from E1-P. Leak from E1-OT was negligible. b) Testbed flow pattern on February 20, 2018. Main producer was E1-P (combined flow from collar). Small flow noticed from E1-OT, and negligible outflow occurred from E1-PDT. c) Testbed flow pattern during post-February 20, 2018. Both E1-P and E1-PDT are main producers with small leaks from E1-OT and E1-PST. The weep near the collar of E1-P consistently seeped during these tests.

5.2 Conceptual Flow Model: 142-Notch

As with the notch-164 activities, observational data (e.g., MEQ, DTS, etc.) combined with dominant flow patterns and fracture systems (Figure 5) in the testbed were used to create a conceptual flow model for notch-142 activities (Figure 18).

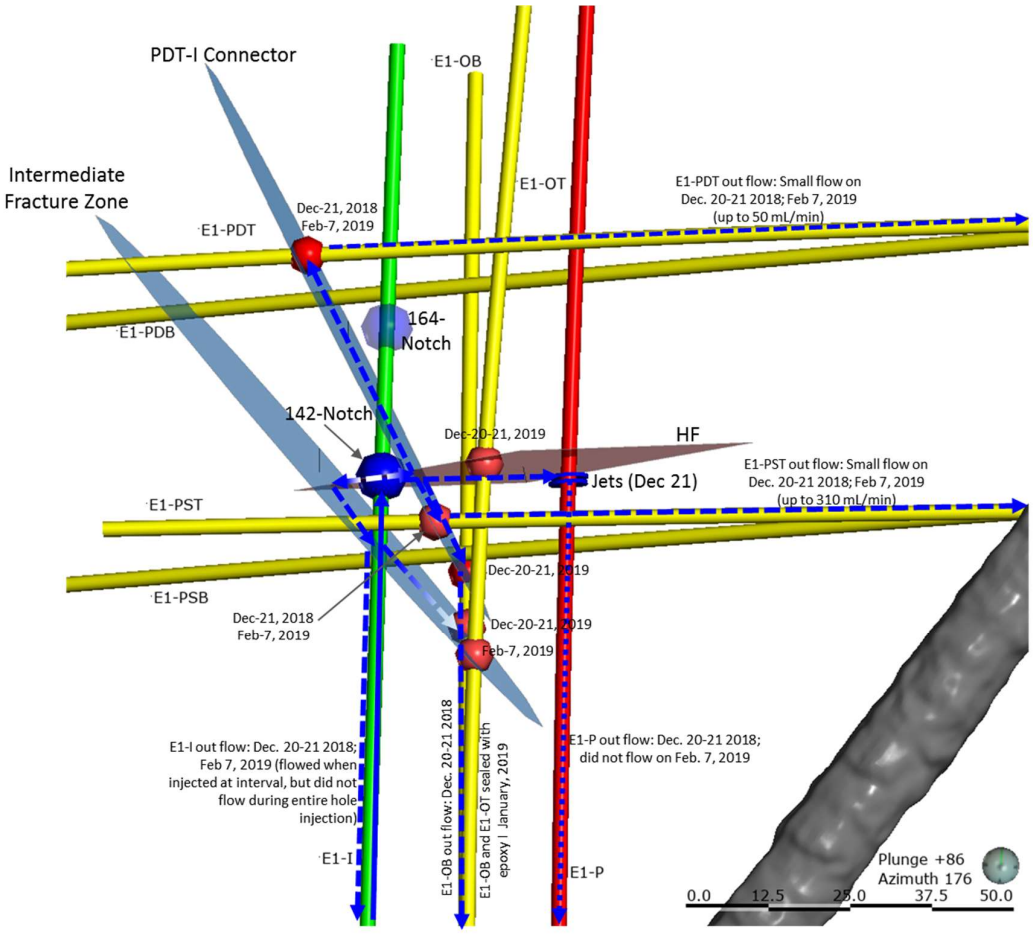

Figure 18. Flow paths in the testbed associated with 142-notch activities. Blue lines with arrowhead indicate the major flow paths in consistent with the temperature anomalies (red spheres) and the outflows recorded at various wells.

6. Conclusions

The EGS Collab project is conducting a series of stimulation and interwell flow tests in an intermediate scale (~10-20 m) testbed located on the 4850 level in the Sanford Underground Research Facility (SURF) in Lead, South Dakota. The testbed consists of eight ~200 ft (~60 m) HQ-diameter (9.6 cm) boreholes. Six boreholes (E1-OT, E1-OB, E1-PST, E1-PSB, E1-PDT, E1-PDB) are intensively instrumented with geophysical sensors and used as monitoring wells. The rest of the two boreholes have remained open, and are being used as injection and production wells. The injection well has been notched at five locations to facilitate and initiate hydraulic fracture. These notches are located approximately at depths of 112 ft, 128 ft, 142 ft, 164 ft, and 182 ft.

Geologically, the testbed is located in graphitic sericite-biotite phyllite/schist of the Ross member of the Poorman Formation. A framework geologic model has been created in Leapfrog for the testbed and its immediate vicinity. Field observation, core inspections, and borehole image interpretation suggest that the testbed is not devoid of natural fractures (contrary to the initial expectation) and consists of several natural fractures: both open and healed fractures. Most of the natural fractures align along NW-SE trending fracture zones. The emplacement of the NW-SE trending Tertiary rhyolite dikes near the testbed seems to

have some structural impact on the natural fracture zone in the testbed. We have identified and mapped at least five natural fracture zones in the testbed: these are the Deep Fracture zone (OT-P Connector), the PDT-OT Connector, the PDT-I Connector, the Intermediate Fracture zone, and the Shallow Fracture zone. Initially, only the Deep Fracture zone showed naturally established cross-borehole hydraulic communication. However, over the course of stimulation and flow tests, other fracture zones were also activated and established some degree of cross-borehole hydraulic connection. Several weeps with the same general orientations are mapped at various locations along the drifts on the 4850 level.

By the end of March 2019, four hydraulic stimulations had been conducted at three of the notches. Distributions of MEQ hypocenters and locations of temperature anomalies and water jets associated with stimulation conducted at the 142-notch and the 164-notch unambiguously suggest the creation of expected hydraulic fractures in the testbed. The hydraulic fractures created at these two notches have steep dips (72-82˚) and near E-W strike (~N80˚E-S80˚W). The attitude of the hydraulic fractures is very similar to the pre-test design orientations of the expected hydraulic fracture controlled by ambient stress field of the testbed. Moreover, as predicted, both of these hydraulic fractures grew eastwards towards the drift from the notches as a response to the stress gradient imposed by drift-cooling induced thermal gradient (Fu et al., 2018).

After the creation of a hydraulic fracture at the 164-notch, a series of hydraulic characterization tests were performed with injection of different water types. Similarly, one series of tracer tests was conducted to characterize the fractures associated with this notch. These hydraulic characterization tests provided significant information to create some early conceptual flow path models for the test bed. Based on the observations of outflow patterns of several monitoring holes and E1-P, the hydraulic fracture from the 164-notch can be opened all the way to E1-P and consistently kept open to sustain a flow through it. However, a significant portion of the water is likely routed to the natural facture zones in the testbed, and a portion of this water is being captured as leaks coming out through some monitoring wells.

The current testbed has undergone at least three phases of change over time. Each of these changes was associated with changes in injection flow rates, activation of the natural fracture zones, and failure of the grout that was supposed to completely seal the monitoring holes. By the end of March 2019, the testbed relevant to 164-notch has been in stable hydraulic condition, and the pressure response and flow patterns are appearing to be repetitive. It is expected that further processing and interpretation of existing data along with new data from the ongoing and planned hydraulic tests (thermal and tracer tests) in the field will help refine our understanding of the testbed. The results and lessons learned through this project are useful and important for the EGS FORGE, and will help make EGS a successful geothermal technology in the future.

Acknowledgement

The research supporting this work took place in whole or in part at the Sanford Underground Research Facility in Lead, South Dakota. Funding for this work is supported by the Office of Science of the Department of Energy under Contract Number DE-AC07-05ID14517 with Idaho National Laboratory. The assistance of the Sanford Underground Research Facility and its personnel in providing physical access and general logistical and technical support is acknowledged. Data related to geology and mine geometry were provided by Kathy Hart (Sanford Underground Research Facility/South Dakota School of Mines and Technology).

The earth model output for this paper was generated using Leapfrog Software. Copyright © Seequent Limited. Leapfrog and all other Seequent Limited product or service names are registered trademarks or trademarks of Seequent Limited. The conditioned stochastic discrete fracture network (CS-DFN) model was created using FracMan software (Golder Associates, Inc.). Discussion with A. Finnila (Golder Associates, Inc.) was helpful in developing approach for creating CS-DFN for the testbed.

REFERENCES

ARUP, 2015. Geotechnical Interpretive Report. FA/A Services for Site Investigation in Support of the LBNF Far Site Conventional Facilities Report. Prepared for the South Dakota Science and Technology Authority.

Caddey, S.W., .L. Bachman, T.J. Campbell, R.R. Reid, and R.P. Otto., 1991. The Homestake Gold Mine, An Early Proterozoic Iron-Formation-Hosted Gold Deposit, Lawrence County, South Dakota, U. S. Geological Survey Bulletin 1857-J, Geology and Resources of Gold in the United States, 67 pp.

Dobson, P., Kneafsey, T.J., Blankenship,D., Valladao, C., Morris, J., Knox, H., Schwering, P., White, M., Doe, T., Roggenthen, W., Mattson, E., Podgorney, R., Johnson, T., Ajo-Franklin, J., and the EGS Collab Team, 2017. An introduction to the EGS Collab project. GRC Transaction, 41, 13 p.

Finnila, A., Forbes, B., and Podgorney, R., 2019. Building and utilizing a discrete fracture network model of the FORGE Utah Site. In Proceedings 44th Workshop on Geothermal Reservoir Engineering, Stanford University, Stanford, California.

Frash, L.P., Carey, J.W., Welch, N.J., and the EGS Collab Team, 2019. EGS Collab Experiment 1 Geomechanical and hydrological properties by triaxial direct shear. Proceedings 44th Workshop on Geothermal Reservoir Engineering, Stanford University, Stanford, California, 11 p.

Fu, P., Schoenball, M., Morris, J., Ajo-Franklin, J., Knox, H.A., Kneafsey, T.J., Burghardt, J., White, M., and the EGS Collab Team. (2019). Microseismic signatures of hydraulic fracturing: a preliminary interpretation of intermediate-scale data from the EGS Collab Experiment. In Proceedings 44th Workshop on Geothermal Reservoir Engineering, Stanford University, Stanford, California.

Fu, P., White, M.D., Morris, J.P., Kneafsey, T.J., and EGS Collab Team, 2019. Predicting hydraulic fracture trajectory under the influence of a mine drift in EGS Collab Experiment I." Proceedings 43rd Workshop on Geothermal Reservoir Engineering, Stanford University, Stanford, California, 11 p.

Hart, K., Trancynger, T.C., Roggenthen, W., and Heise, J., 2014. Topographic, geologic, and density distribution modeling in support of physics experiments at the Sanford Underground Research Facility (SURF). Proceedings of the South Dakota Academy of Science, 93, 33-41.

Heise, J., 2015. The Sanford underground research facility at Homestake. Journal of Physics: Conference Series, 606(1), 26 p.

Huang, H., Neupane, G., Podgorney, R., Mattson, E., & the EGS Collab Team, 2019. Mechanistically modeling of hydraulic fracture propagation and interaction with natural

fractures at EGS-Collab Site. In Proceedings 44th Workshop on Geothermal Reservoir Engineering, Stanford University, Stanford, California.

Johnson, T., C. Strickland, H. Knox, J. Thomle, V. Vermuel, C. Ulrich, T. Kneafsey, D. Blankenship, and EGS Collab Team, 2019. EGS Collab project electrical resistivity tomography characterization and monitoring status. In Proceedings 44th Workshop on Geothermal Reservoir Engineering, edited, Stanford University, Stanford, California.

Kneafsey, T.J. and Dobson P.F., Ajo-Franklin, J.B., Guglielmi, Y., Valladao, C.A., Blankenship, D.A., Schwering, P.C., Knox, H.A., White, M.D., Johnson, T.C., Strickland, C.E., Vermuel V.R., Morris, J.P., Fu, P., Mattson, E., Neupane, G., Podgorney, R.K., Doe, T.W., Huang, L., Frash, L.P., Ghassemi, A., Roggenthen, W., and the EGS Collab Team, 2019a. EGS Collab Project: Status, Tests, and Data. ARMA-19-2004, p. 21.

Kneafsey, T.J. et al., 2019b. EGS Collab Project Overview Paper. In preparation.

Knox, H., Fu, P., Morris, J., Guglielmi, Y., Cook, P., Herrick, C., Lee, M., Ajo-Franklin, J., Su, J.C., and the SIGMA-V Team, 2017. Fracture designs for the Collab/SIGMA-V project. GRC Transaction, 41, 9 p.

Lisenbee, A.L. and Terry, M., 2009. Development of a 3-D structural geology model of Homestake's 4100 to 5000 levels at the proposed location of the large cavities. South Dakota School of Mines and Technology, SDSMT Contract # 09-05, 38 pp.

Mattson, E.D., Neupane, G., Plummer, M.A., Hawkins, A., Zhang, Y. and the EGS Collab Team 2019. Preliminary Collab fracture characterization results from flow and tracer testing efforts. In Proceedings 44th Workshop on Geothermal Reservoir Engineering, edited, Stanford University, Stanford, California.

Morris, J.P., Dobson, P., Knox, H., Ajo-Franklin, J., White, M.D., Fu, P., Burghardt, J., Kneafsey, T.J., Blankenship, D., and the EGS Collab Team, 2018. Experimental design for hydrofracturing and fluid flow at the DOE Collab testbed. Proceedings, 43rd Workshop on Geothermal Reservoir Engineering, Stanford University, (2018) 11 p.

Oldenburg, C.M., P.F. Dobson, Y. Wu, P.J. Cook, T.J. Kneafsey, S. Nakagawa, C. Ulrich, D.L. Siler, Y. Guglielmi, J. Ajo-Franklin, J. Rutqvist, T.M. Daley, J.T. Birkholzer, H. Wang, N.E. Lord, B.C. Haimson, H. Sone, P. Vigilante, W.M. Roggenthen, T.W. Doe, M.Y. Lee, M. Ingraham, H. Huang, E.D. Mattson, J. Zhou, T.J. Johnson, M.D. Zoback, J.P. Morris, J.A. White, P.A. Johnson, D. DD. Coblentz, and J. Heise, 2016. Intermediate-Scale Hydraulic Fracturing in a Deep Mine, kISMET Project Summary 2016, Lawrence Berkeley National Laboratory, LBNL-1006444.

Roggenthen, W.M., T.W. Doe, and the EGS Collab team. 2018. Natural Fractures and Their Relationship to the EGS Collab Project in the Underground of the Sanford Underground Research Facility (SURF). In Proceedings, 52nd US Rock Mechanics / Geomechanics Symposium, American Rock Mechanics Association, ARMA 18-1190, 9 p.

Schoenball, M., Ajo-Franklin, J., Blankenship, D., Cook, P., Dobson, P., Guglielmi, Y., Fu, P., Kneafsey, T., Knox, H., Petrov, P., and Robertson, M., Schwering, P., Templeton, D., Ulrich, C., Wood, T., and the EGS Collab Team, 2019. Microseismic monitoring of meso-scale stimulations for the DOE EGS Collab project at the Sanford Underground Research Facility. In Proceedings: 44th Workshop on Geothermal Reservoir Engineering, Stanford University, Stanford, CA.

Schwering, P.C., Knox, H.A., Hoots, C.R., Linneman, D., Ajo-Franklin, J., and the EGS Collab team, 2018. The EGS Collab Hydrofracture Experiment at the Sanford

Underground Research Facility – Campaign Cross-Borehole Seismic Characterization. GRC Transactions, 42, 10 p.

Singh, A., Zoback, M., Neupane, G., Dobson, P.F., Kneafsey, T.J., Schoenball, M., Guglielmi, Y., Ulrich, C., Roggenthen, W., Uzulnar, N., Morris, J., Fu, P., Schwering, P.C., Knoz, H.A., Frash, L., Doe, T.W., Wang, H., Condon, K., Johnston, B., and the EGS Collab Team, 21019. Slip Tendency Analysis of Fracture Networks to Determine Suitability of Candidate Testbeds for the EGS Collab Hydroshear Experiment. GRC Transactions, v. 43.

Steadman, J.A., and Large, R.R., 2016. Synsedimentary, Diagenetic, and Metamorphic Pyrite, Pyrrhotite, and Marcasite at the Homestake BIF-Hosted Gold Deposit, South Dakota, USA: Insights on Au-As Ore Genesis from Textural and LA-ICP-MS Trace Element Studies." Economic Geology, 111, 1731-1752.

Ulrich, C., Dobson, P.F., Kneafsey, T.J., Roggenthen, W.M., Uzunlar, N., Doe, T.W., Neupane, G., Podgorney, R., Schwering, P., Frash, L. and Singh, A., 2018. The distribution, orientation, and characteristics of natural fractures for Experiment 1 of the EGS Collab Project, Sanford Underground Research Facility. In Proceedings, 52nd US Rock Mechanics/Geomechanics Symposium, American Rock Mechanics Association, ARMA 18-1252, 8 p.

White, M., Fu, P., Huang, H., Ghassemi, A., and EGS COLLAB Team, 2017. The Role of Numerical Simulation in the Design of Stimulation and Circulation Experiments for the EGS Collab Project. GRC Transaction, 41, 18 p.

White, M., T. Johnson, T. Kneafsey, D. Blankenship, P. Fu, H. Wu, A. Ghassemi, J. Lu, H. Huang, G. Neupane, C. Oldenburg, C. Doughty, B. Johnston, P. Winterfeld, R. Pollyea, R. Jayne, A. Hawkins, Y. Zhang, and EGS Collab Team, 2019. The Necessity for Iteration in the Application of Numerical Simulation to EGS: Examples from the EGS Collab Test Bed 1, in 44th Workshop on Geothermal Reservoir Engineering, edited, Stanford University, Stanford, California.

Williams, C.F., Reed, M.J., Mariner, R.H., DeAngelo, J., and Galanis, S.P. Jr., 2008. Assessment of moderate- and high-temperature geothermal resources of the United States. US Department of the Interior, US Geological Survey, Fact Sheet 2008-3082.